2D and thin-film copper synthesized via magnetron sputtering

Bin Gu[a], Guangyu Wen[a], Bo Zhang[a *], Janicek Petr[b,c], Tomas Wagner[c,d*]

[a]College of Physics, Hebei Normal University, Shijiazhuang 050024, China
[b]Institute of Applied Physics and Mathematics, Faculty of Chemical Technology, University of Pardubice, Studentska 95, Pardubice 530 02, Czech Republic
[c]Center of Materials and Nanotechnologies, Faculty of Chemical Technology, University of Pardubice, nam. Cs. Legii 565, Pardubice 530 02, Czech Republic
[d]Department of General and Inorganic Chemistry, Faculty of Chemical Technology, University of Pardubice, Studentska 573, 532 10 Pardubice, Czech Republic

Abstract

Two-dimensional metals have gained great attention in recent years. However, most of these metals possess relatively strong chemical bonding in three directions; therefore, it is difficult to synthesize 2D metals. In this paper, we prepared 2D and thin-film copper materials via magnetron sputtering. 2D and thin-film copper are formed due to the accumulation of strain and stress associated with different coefficients of thermal expansion for the metal and substrate. SEM and AFM studies suggest that the minimum thickness of a freestanding single layer is approximately 1 nm, with lateral dimensions up to a few millimeters.

Keywords: 2D materials; thin film; metal

1. Introduction

Two-dimensional metals have been widely studied in many fields[1–7,] where the utilization of various 2D metals is also predicted. Nevertheless, most of these metals possess relatively strong chemical bonding in three directions, leading to great challenges in synthesizing them into ultrathin 2D monolayers[8]. Since the atomic bonding in metals is naturally three dimensional, 2D metals are generally different from other types of 2D materials. Due to the issue of thermodynamic stability, the lateral size of 2D metals is restricted. Thus, large aspect ratios (lateral scale/thickness) distinguish 2D metals from their bulk counterparts[9]. Thus, an ultrathin metal film with a large lateral scale deposited by a magnetron sputter could be considered a 2D metal. Wang *et al*. prepared freestanding metallic 2D layers, with a thickness of ~21 nm and a large lateral scale, via direct current (DC) magnetron sputtering, which is referred to as polymer surface buckling enabled exfoliation (PSBEE)[10]. In comparison with other methods, the method utilizing magnetron sputtering is simple and effective. However, the growth of material during magnetron sputtering follows the rule of the Volmer–Weber mode, in which isolated islands grow to join into thin films[11]. According to the literature, the minimum thickness of a nonporous sputtered thin film must be ~10 nm. Once the thickness is lower than 10 nm, excessive porosity may appear[12].

Wet chemical synthesis is one of the most common methods for preparing 2D metals[13]. Researchers have successfully synthesized many different 2D metals, including silver[14], gold[15], and lead[16], with the help of specific chemical agents. However, chemical synthesis methods have several disadvantages: the efficiency of synthesis is rather low, and the lateral size of the 2D flake is relatively small[13]. In addition to chemical synthesis, molecular beam epitaxy (MBE) is another promising method for fabricating 2D metals. However, MBE suffers from low productivity. Consequently, there is a high demand for developing an alternative method to synthesize 2D metals at a low cost[17].In previous studies, we developed a new method for fabricating 2D materials via thermal evaporation and magnetron sputtering. 2D $GeSe_2$ was first synthesized by thermal evaporation[18]. Afterwards, 2D $Ge_2Sb_2Te_5$ was prepared via magnetron sputtering [19]. In subsequent research, 2D tungsten was successfully deposited in a similar way [20].

In this paper, we modulate the morphology of sputtered material from thin film to 2D material by controlling the temperature

of the substrate. The thickness of a single layer is approximately 1 nm. Moreover, the lateral size of the freestanding 2D single layer is a few millimeters. The formation of 2D metals depends on the presence of stress-related defects.

2. Experiment

The as-deposited copper samples are classified into two types (2D, thin film) according to their structure. Both samples were prepared via magnetron sputtering, in which an RF sputtering power of 30 W and argon gas flow were utilized. During the sputtering deposition processes, the background pressure is typically 1×10^{-4} Pa, and the working pressure is 1 Pa. Both samples were sputtered for 30 mins. The substrate-target distance was maintained at 60 mm (2D) and 78 mm (thin film). In addition to the larger substrate-target distance, additional cooling was also applied to the thin-film copper substrate via a cooling kit. The cooling kit included a steel holder and mask that transferred heat from the substrate. The experimental setup is shown in Fig. S1 and Table S1. Subsequently, the 2D copper samples were transferred to a beaker with distilled water and a vacuum furnace for further exfoliation.

The top and cross-sectional morphologies were characterized by a HITACHI S-4800 scanning electron microscope (SEM). The topography and current spread mapping were performed by a Bruker multimode VIII/Bruker Dimension Icon, respectively. The freestanding flakes of copper were studied by a JEM-F200 JEOL high-resolution transmission electron microscope (HRTEM). The spatial distributions of the temperature and mechanical stress within the Cu layer (with a thickness ~ 200 nm) on the Si substrate (with dimensions of 5 mm × 5 mm × 0.5 mm) were obtained using COMSOL 6.1 via the finite element method. A 2D model representing the side view was adopted. The spatial distribution of temperature (T) can be calculated from the general heat transfer equation using the heat transfer module:

$$d_z \rho C_p \vec{v} \cdot \nabla T + \nabla \cdot \vec{q} = d_z Q + q_0 + d_z Q_{ted}$$

$$\vec{q} = -d_z k \nabla T$$

where the right part of the first equation contains additional heat sources Q (W/m^3), namely, Q_{ted} (W/m^3), with thermoelastic damping accounting for thermoelastic effects in solids and q_0 (W/m^2) being the inward heat flux. Additionally, d_z (m) is the thickness of the domain in the out-of-plane direction (d_z = 5 mm), ρ (kgm^{-3}) for density, C_p (Jkg^{-1}K^{-1}) for specific heat capacity at constant pressure, $\vec{v}$ (m/s) for fluid velocity vector, $\vec{q}$ (W/m^3) for conductive heat flux and k (Wm^{-1}K^{-1}) for thermal conductivity. The boundary conditions are constant temperatures (46 °C on top of the Cu layer, 43 °C at the interface between Si and Cu and 40 °C on the bottom of the Si substrate) together with thermal insulation on the left and right boundaries.

To include thermal expansion, a structural mechanics module was utilized. Here, the local strain ε defined using the local displacement vector $\vec{u}$ depends on the coefficient of thermal expansion CTE as

$$\varepsilon = CTE(T) \cdot dT = \vec{\nabla} \cdot \vec{u}$$

The values of stress are consequently calculated from Hooke's law. For structural mechanics, all boundaries can freely move. The parameters for the COSMOL simulation are shown in Table S2.

3. Results and Discussion

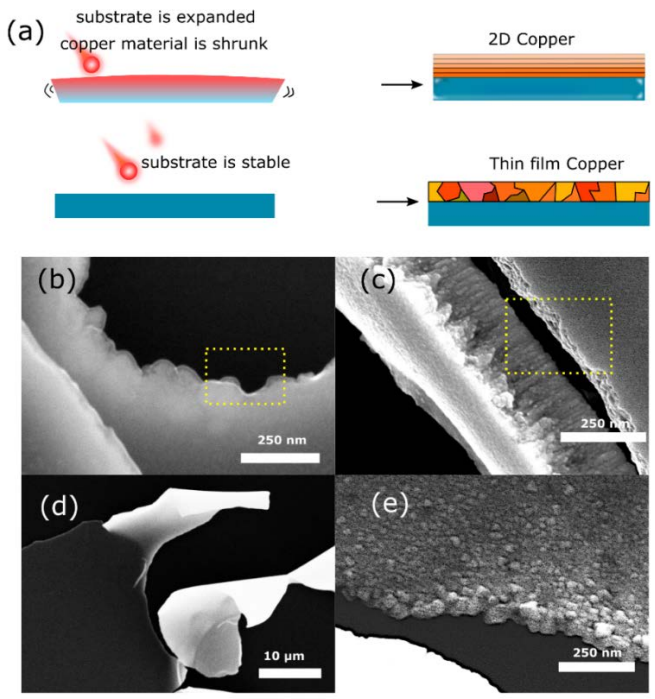

Fig. 1. (a) Graphical illustration of the formation of 2D and thin-film copper; (b)-(c) the morphology of 2D copper after ultrasonic exfoliation, where the single layers are shown in the yellow square; (d)-(e) the morphology of thin-film copper after sonication.

In our previous studies, we successfully synthesized 2D $Ge_2Sb_2Te_5$ and 2D tungsten via radiofrequency magnetron sputtering[21]. However, the underlying mechanism was not discussed in depth in these papers. In this paper, we propose a model that explains the formation of 2D and thin film materials prepared via magnetron sputtering, as shown in Fig. 1(a). In principle, the process of magnetron sputtering consists of 3 steps: (1) vaporization of the target material; (2) the migration and collision of atoms, molecules, and ions; and (3) deposition of atoms and molecules on the substrate[22]. Since the silicon substrate and material have different coefficients of thermal expansion, thermal stress accumulates in the as-deposited material after deposition. Furthermore, stress-related defects create the structure of 2D copper. To obtain thin-film copper, we minimized the thermal expansion of the substrate during deposition by increasing the target-to-substrate distance and applying a cooling kit.

Both copper materials (film and 2D structure) were sonicated in a water bath for exfoliation, which is referred to as the wet exfoliation method in this paper. For traditional 2D materials, chemical or physical treatment weakens interlayer van der Waals interactions among single layers, resulting in single-layered nanosheets. The sonication method is one of the most common exfoliation methods, in which generated cavities offer a large driving force for the exfoliation of 2D materials[23]. Likewise, 2D copper was exfoliated via a similar principle in which defects, created inside 2D copper during the deposition and cooling process, might play a crucial role. Under the impact of microjets and shock waves generated by the collapse of cavities, the propagation of defects facilitates the separation of adjacent Cu single layers. The SEM images in Fig. 1(b) and (c) show the morphology of the 2D copper film after wet exfoliation, where single layers are present at the edge of the sample (in the yellow square). When cooling was applied using a cooling kit, thin-film copper was formed without ultrathin single layers, as shown in Fig. 1(d) and (e). However, a high density of grains is clearly observed in thin-film copper, which restricts the conductivity of the thin film[12]. In summary, the SEM images confirm the validity of the structural model, where the selective deposition of 2D and thin-film copper is a potential way to improve, e.g., the quality of metal interconnect in integrated circuits.

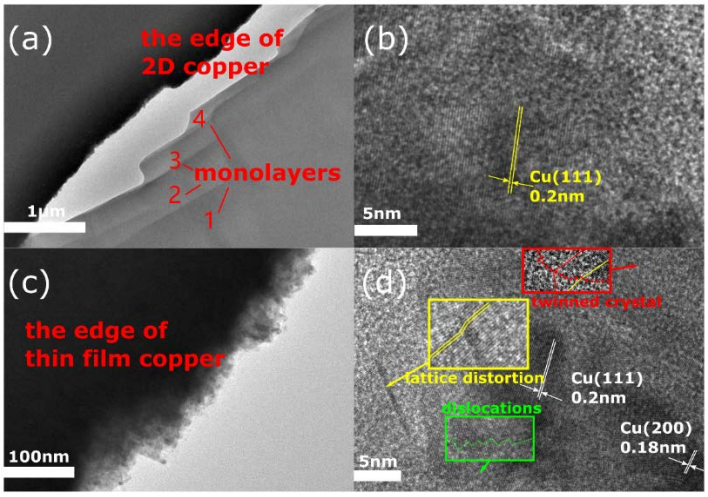

Fig. 2. HRTEM images of thin-film and 2D copper, where the interplanar spacing and defects are marked: (a) single layers of 2D copper; (b) the crystalline lattice enlarged from (a); (c) morphology of thin-film copper; (d) the crystalline lattice enlarged from (c).

For HRTEM imaging, copper flakes were scratched from the substrate and transferred to a copper grid in an ethanol solution. The HRTEM images of 2D and thin-film copper are presented in Fig. 2. In Fig. 2(a), a stack of single layers at the edge of the flake is shown. The crystalline structure of a single layer is dominated by the (111) plane, as shown in Fig. 2(b)[24]. The morphology of the thin-film copper shown in Fig. 2(c) does not present a structure with single layers. However, the HRTEM image of the thin-film copper in Fig. 2(d) shows various defects. First, the persistent kink bands represent a lattice distortion marked in the yellow square of Fig. 2(d). Such deformation bands often appear due to unidirectional plastic strains in local regions[25]. Second, a twinned crystal is shown in the red square of Fig. 2(d), which is formed by the slipping of planes. Moreover, helix dislocations are marked as a zigzag line in the green square in Fig. 2(d) (the original image is shown in Fig. S2). The formation of helix dislocations is closely related to the climb of edge dislocations and the glide of screw dislocations[26]. We believe that the defects in the thin film are closely related to the grain boundaries, which is consistent with the results shown in Fig. 1e. In brief, 2D copper has a lower density of crystalline boundaries as well as defects, facilitating the exfoliation of ultrathin single layers.

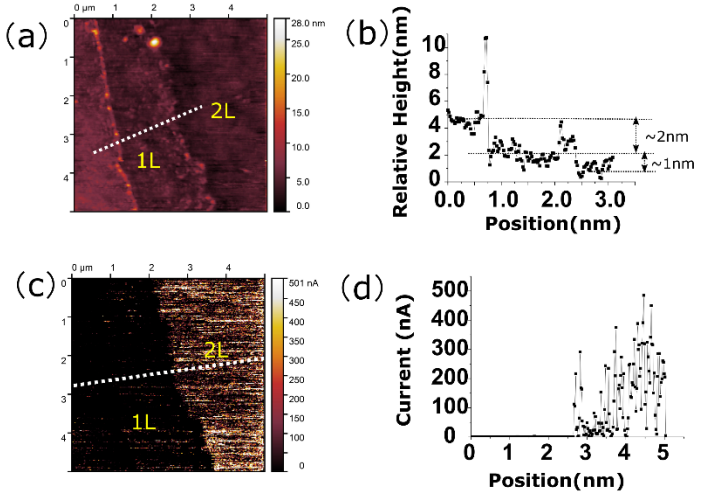

Fig. 3. (a) Topographic image of 2D copper after ultrasonic exfoliation taken by conductive AFM; (b) profile of (a) at the position of the dashed line; (c) spread current map of (a) taken by conductive AFM; (d) profile of the current distribution at the position of the dashed line.

In this paper, 2D copper was exfoliated via sonication. After a duration of sonication, the flakes were exfoliated and dispersed in water. Consequently, the flakes were transferred from the solution to the silicon wafer, as shown in Fig. S3. Under an optical

microscope, the ultrathin freestanding flake of 2D copper is transparent with a large lateral size, showing an advantage for future applications. Afterwards, the conductivity and topography map of the flakes were studied via conductive AFM. The topographic map of the flake in Fig. 3(a) shows two single layers, with the thickness of the single layer being approximately 1-2 nm (as shown in Fig. 3(b)). This thickness is clearly much thinner than the minimum thickness of a metallic thin film in theory. The corresponding spread current map in Fig. 3(c) and profile in Fig. 3(d) reveal an interesting result in which the current is lower in each freestanding single layer (1 L, 2 L). In other words, the number of single layers determines the overall conductivity of 2D copper. This finding provides a new way to regulate the conductivity of 2D metals in a precise way. Thus, 2D metals offer a new choice for metal interconnect materials in microelectronic circuits.

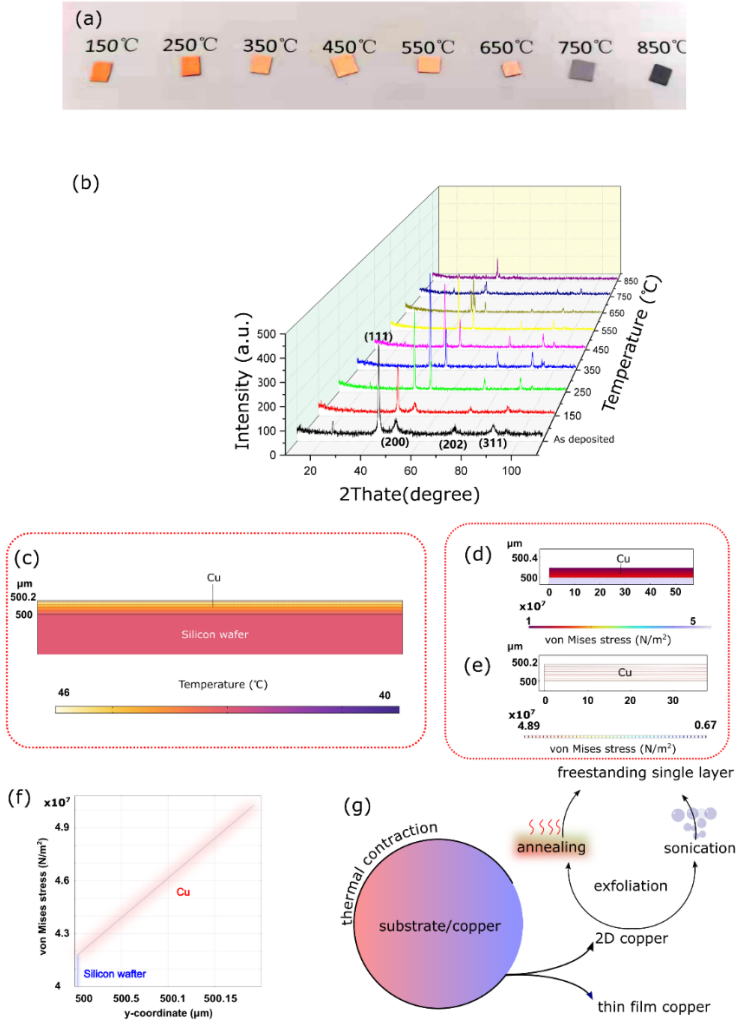

Fig. 4 (a) Changes in the appearance of 2D copper after thermal exfoliation; (b) XRD pattern of 2D copper after thermal exfoliation; (c) the distribution of temperature with iso-temperature lines; (d) distribution of the stress inside the substrate and Cu layer with iso-stress lines; (e) enlarged view from (d) with iso-stress lines; (f) dependence of the stress values on the *y*-coordinate (i.e., distance from the bottom of the sample); (g) the experimental mechanism for 2D and thin-film copper.

The 2D copper samples were annealed in a vacuum furnace from 150 ℃ to 850 ℃ for an hour. After annealing at 850 ℃, a visible gap appears between the single layers of 2D copper, as shown from the AFM topography map in Fig. S4. The gap between single layers further induces light interference, and the material changes to a dark black shape, as shown in Fig. 4(a). The crystal structures of annealed 2D copper were characterized by XRD in Fig. 4(b), and the peak corresponding to Cu (111) appears at 44°C, which is consistent with the standard JCPDS Card No. 96-500-2017, suggesting that no phase change occurs during the thermal exfoliation process [27].

As discussed above, the formation of 2D copper is assumed to be related to the accumulation of stress during the cooling process of the as-deposited material and silicon wafer after deposition. The COSMOL simulations of the temperature

distribution and von Mises stress further suggest that the stress induced by temperature variation possibly shapes the as-deposited copper into a multilayered structure. The thickness of the as-deposited copper was set to 200 nm, and the lateral dimensions were 5 mm × 5 mm. The temperature of the copper was set at 46°C at the beginning of cooling, which reached the ambient temperature (25°C) at the end of the simulation. At the beginning of cooling, the iso-thermal lines are parallel to the interface between the copper and silicon inside the as-deposited copper, as shown in Fig. 4(c). The distribution of stress in the final equilibrium state is shown in Fig. 4 (d) and (e), where the iso-stress lines are parallel to the interface. From the stress profile across the as-deposited copper and silicon wafer, the von Mises stress increases with the thickness of the as-deposited copper, as shown in Fig. 4(f). As a result, the sheer stress can cause plastic deformation inside the as-deposited copper. During the exfoliation process, plastic deformation further led to the development of large cracks separating the adjacent freestanding single layers, as shown in Fig. 4(g).

4. Conclusion

In this paper, we prepared a 2D copper material via magnetron sputtering. The structure of the deposited materials is governed by the temperature of the silicon substrate, which results in the formation of a thin film using a cooling kit. In our opinion, the inherent mechanism is described as the accumulation of stress, which is supported by COMSOL simulation. In general, this approach is a universal method for preparing many different 2D metals. A single layer of metal is transparent with a thickness of 1-2 nm, and the lateral size of the freestanding layers is a few millimeters. All these findings open a new study of 2D materials where this method has many unique advantages over other methods. In the future, many different types of metals, including alloys, are expected to be synthesized with the contribution of magnetron sputtering.

Funding

The author thanks for financial support from the grant of the Ministry of Education, Youth- and Sports of Czech Republic (grant LM2023037), the European Regional Development Fund Project, the project NANOMAT CZ.02.1.01/0.0/0.0/17_048/0007376 and the project of Faculty of Chemical Technology, University of Pardubice “Excellent teams”2023, the grant of Hebei Normal University (L2021B12) and the HeBei NSF (QN2023054)

Competing Interests

The authors declare that they have no conflict of interest.

Research Data Policy and Data Availability Statements

The data that support the findings of this study are available on request from the corresponding author, upon reasonable request.

Author Contribution

Guangyu Wen and Bin Gu carried out the experiment. Petr Janicek conducted COMSOL simulation. Bo Zhang wrote the manuscript with support from Tomas Wagner. Tomas Wagner supervised the project.

Reference

1. Chen, Y. *et al.* Two-Dimensional Metal Nanomaterials: Synthesis, Properties, and Applications. *Chemical Reviews* **118**, 6409–6455 (2018).
2. Liu, X., Ren, J.-C., Shen, T., Li, S. & Liu, W. Lateral InSe p–n Junction Formed by Partial Doping for Use in Ultrathin Flexible Solar Cells. *J Phys Chem Lett* **10**, 7712–7718 (2019).
3. Dong, K. *et al.* Constructing efficient ternary PtTeCu nano-catalysts with 2D ultrathin-sheet structures for oxidation reaction of alcohols. *Appl Surf Sci* **609**, 155301 (2023).
4. Wang, H. *et al.* Interlayer-expanded 2D VS_2 for fast response/recovery NO_2 detection at low-temperature. *Appl Surf Sci* **606**, 154894 (2022).
5. Du, C. *et al.* Synthesis of ultra-thin 2D MnO_2 nanosheets rich in oxygen vacancy defects and the catalytic oxidation of

n-heptane. *Appl Surf Sci* **606**, 154846 (2022).
6. Hwang, S. *et al.* A facile approach towards Wrinkle-Free transfer of 2D-MoS_2 films via hydrophilic Si_3N_4 substrate. *Appl Surf Sci* **604**, 154523 (2022).
7. Liu, J., Shen, T., Ren, J.-C., Li, S. & Liu, W. Role of van der Waals interactions on the binding energies of 2D transition-metal dichalcogenides. *Appl Surf Sci* **608**, 155163 (2023).
8. Fan, Z., Huang, X., Chen, Y., Huang, W. & Zhang, H. Facile synthesis of gold nanomaterials with unusual crystal structures. *Nat Protoc* **12**, 2367–2376 (2017).
9. Lin, B. *et al.* Centimeter-Scale Two-Dimensional Metallenes for High-Efficiency Electrocatalysis and Sensing. *ACS Mater Lett* **5**, 397–405 (2023).
10. Wang, T. *et al.* The controlled large-area synthesis of two dimensional metals. *Materials Today* **36**, 30–39 (2020).
11. Lazzari, R. & Jupille, J. Silver layers on oxide surfaces: morphology and optical properties. *Surf Sci* **482–485**, 823–828 (2001).
12. Zhang, C. *et al.* An ultrathin, smooth, and low-loss Al-doped Ag film and its application as a transparent electrode in organic photovoltaics. *Advanced Materials* (2014) doi:10.1002/adma.201306091.
13. Wang, T., Park, M., Yu, Q., Zhang, J. & Yang, Y. Stability and synthesis of 2D metals and alloys: a review. *Mater Today Adv* **8**, 100092 (2020).
14. Kim, M. H. *et al.* Maneuvering the growth of silver nanoplates: use of halide ions to promote vertical growth. *J. Mater. Chem. C* **2**, 6165–6170 (2014).
15. Fan, Z. *et al.* Stabilization of 4H hexagonal phase in gold nanoribbons. *Nat Commun* **6**, 7684 (2015).
16. Huang, X. *et al.* Freestanding palladium nanosheets with plasmonic and catalytic properties. *Nat Nanotechnol* **6**, 28–32 (2011).
17. Li, L. *et al.* Two-dimensional transition metal honeycomb realized: Hf on Ir(111). *Nano Lett* **13**, 4671–4674 (2013).
18. Zhang, B. *et al.* 2D $GeSe_2$ amorphous monolayer. *Pure and Applied Chemistry* **91**, 1787–1796 (2019).
19. Zhang, B. *et al.* A layered $Ge_2Sb_2Te_5$ phase change material. *Nanoscale* **12**, 3351–3358 (2020).
20. Zhang, B. *et al.* 2D metallic tungsten material. *Appl Surf Sci* **530**, 147231 (2020).
21. Zhang, B. *et al.* The Structural Modulation of Amorphous 2D Tungsten Oxide Materials in Magnetron Sputtering. *Adv Mater Interfaces* **9**, 2201790 (2022).
22. Gao, P., Meng, L. J., dos Santos, M. P., Teixeira, V. & Andritschky, M. Influence of sputtering power and the substrate–target distance on the properties of ZrO_2 films prepared by RF reactive sputtering. *Thin Solid Films* **377–378**, 557–561 (2000).
23. Huo, C., Yan, Z., Song, X. & Zeng, H. 2D materials via liquid exfoliation: a review on fabrication and applications. *Sci Bull (Beijing)* **60**, 1994–2008 (2015).
24. Sennour, M., Lartigue-Korinek, S., Champion, Y. & Hÿtch, M. J. HRTEM study of defects in twin boundaries of ultra-fine grained copper. *Philosophical Magazine* **87**, 1465–1486 (2007).
25. Ma, T., Miyazawa, T. & Fujii, T. Crystallographic features of deformation-kink bands in coplanar-double-slip-oriented copper single crystals. *Mater Charact* **177**, 111151 (2021).
26. Liu, F., Liu, Z., Lin, P. & Zhuang, Z. Numerical investigations of helical dislocations based on coupled glide-climb model. *Int J Plast* **92**, 2–18 (2017).
27. Qiu, H., Wang, F., Wu, P., Pan, L. & Tian, Y. Structural and electrical properties of Cu films deposited on glass by DC magnetron sputtering. *Vacuum* **66**, 447–452 (2002).